NTNU – Trondheim
Norwegian University of
Science and Technology

Development of high efficiency Axial Flux Motor for Shell Eco-marathon

John Ola Buøy

Master of Energy and Environmental Engineering
Submission date: June 2013
Supervisor: Robert Nilssen, ELKRAFT

Norwegian University of Science and Technology
Department of Electric Power Engineering

Abstract

In 2011 Lubna Nasrin designed an optimized in-wheel axial flux motor for the competition Shell Eco-Marathon. A motor was built for the 2012 competition by Fredrik V. Endresen. Testing of this motor showed however that the performance was nothing like the one anticipated by Nasrin. The conclusion was that the production methods were not good enough and this was the main reason for the poor result.

A new motor was built for use in the 2013 competition. Several design improvements over the old motor which was built in 2010 has been made. Litz wire is used in the stator and Halbach array permanent arrangement in the rotors. Rims, axle and other mechanical parts have also been made brand new this year to try to make the best possible design.

The assembly didn't go without problems, but in the end the motor was fit to the car and tested. It was used in the competition where the team ended up with a third place in the battery electric class.

Several tests were performed on the motor to identify how well it performed compared to the FEM results. Question marks have however been raised when it comes to the results of the test due to problems aligning the motor in the test bench. The results indicate rather high rotational losses, but also an induced voltage 35% lower than anticipated. This should not be critical though as the theoretical efficiency, rotational losses discarded, still is 99% with this value.

The high eddy current and friction losses measured do however ruin the real efficiency of the machine.

Sammendrag

I 2011 designet Lubna Nasrin en optimalisert aksial fluks motor for bruk i Shell Eco-Marathon. Fredrik V. Endresen bygde en motor i 2012 basert på dette designet. Testene som ble utført viste derimot at ytelsen ikke var i nærheten av det som Lubna hadde estimert. Det ble konkludert med at produksjonsmetodene var for dårlige og dette var hovedårsaken til det heller dårlige resultatet.

En ny motor ble bygd for konkurransen i 2013. I forhold til den gamle motoren som ble bygd i 2010 har det nye designet mange forbedringer. Statorviklingene består av Litz wire og permanentmagnetene er bygd opp som et Halbach array. Alt ble bygd nytt i år, felger, aksling og andre mekaniske deler for å kunne optimalisere mest mulig.

Byggingen skulle dog vise seg å bli en utfordring også i år, men motoren ble ferdig og testet på bilen. Den ble brukt i 2013 konkurransen der årets team endte med en tredjeplass i den batterielektriske klassen.

Flere tester ble utført for å kartlegge ytelsen på den nye motoren sammenlignet med designet. Resultatene ble dessverre ikke helt til å stole på da det viste seg vanskelig å få satt motoren riktig opp i testbenken. Rotasjonstapene er mye større enn beregnet og ødelegger virkningsgraden på motoren. Også den motinduserte spenninga er lavere enn beregnet med 35 %. Dette i seg selv skal likevel ikke være kritisk fordi den teoretiske virkningsgraden er fremdeles 99 % med denne verdien når rotasjonstapene er neglisjert.

List of figures

List of symbols

T	Torque
P	Power
I	Phase current
ω	Rotational speed rad/s
e	Induced voltage
n	Rotational speed rpm
Stw	Stator thickness
D_o	Outer diameter of magnet ring
D_i	Inner diameter of magnet ring
k_D	Diameter ratio
λ	Flux linkage
t	time
B	Magnetic field strength
A	Area
μ_0	Permeability in vacuum
P_c	Permeance coefficient
l_m	Equivalent magnet length
A_g	Equivalent air gap area
g	Equivalent air gap length
A_m	Equivalent magnet area
σ	Electric conductivity
B_r	Remanent flux density
l	Slot length
w	Average slot width
R	Electrical resistance
F	Force
k_f	Friction coefficient
$d_{bearing}$	Equivalent diameter of ball bearing
c_f	Air drag coefficient
ρ	Mass density
R	Radius

Contents

Introduction

In the 2011 spring semester Lubna Nasrin designed an optimized axial flux motor for the DNV Fuel Fighter as her master thesis [1]. This design incorporated several improvements over the previous one, like carbon fiber rotor plates, Halbach permanent magnet arrangement, the use of Litz wire in the stator winding and a more precise simulation model to ensure the motor would get the designed back EMF. Her design basically showed half the weight compared to the previous motor and an efficiency of over 97%, a number which also encounters the friction losses.

Nasrin's design was a very good basis for the 2012 team to work with.

A high efficiency propulsion system is much needed for the car to be competitive. Therefore the 2012 team decided to build a motor based on the design of Nasrin. Figure 1 shows the end result of this work. Sadly the production proved to be more difficult than they anticipated and the result was not good enough to be used in the competition [2]. That being said, the work that Fredrik V. Endresen put into this attempt shows the possibility with a design like this and maybe most importantly he has discovered several aspect when it comes to the physical interpretation of a design which might not be easy and therefore the effort needed in this part of project should not be underestimated.

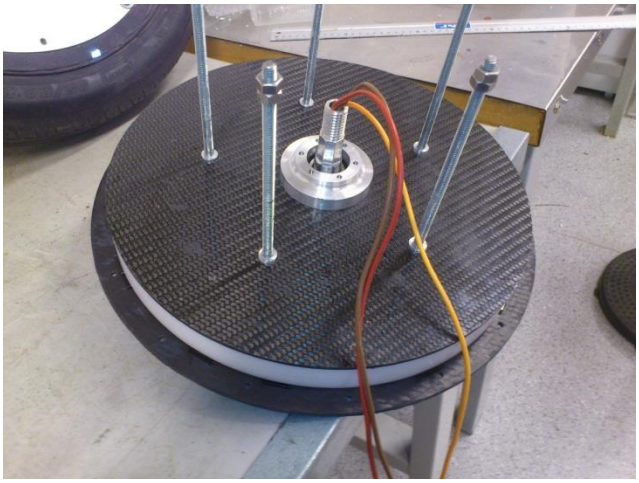

Figure 1: The 2012 motor.

Is it possible to build a motor with such a high efficiency?

A car named Aurora had a similar motor built for a similar type of competition in Australia. It's about building a solar powered car which should drive across the continent. They developed a motor with similar technology as the 2012 motor and achieved an efficiency of 97.9% [3], [4]. That is however without rolling friction. They say the rolling friction belongs to the wheel, not the motor itself. With friction included the same motor was tested to an efficiency of 95.7% [5]. Nasrin's design takes rolling friction into account, but it looks like she has underestimated the value for this loss, which will be explained later in the test results.

This year there have been more focus on the production process, and some of the mechanical students have been directly involved in the motor project. They do have more experience with materials, the use of machines and industrial manufacturing methods and are able to provide help for practical problems.

2013 Design

Like the 2010-2012 motors the 2013 car featured an in-wheel axial flux motor. This type of motor is better suited for low speed direct drive than similar radial flux machines [6] and [7].

The team decided to go with a single motor configuration. Due to lack of resources and time restrictions not very large modifications could be done to the motor controller and therefore the double motor configuration was abandoned. For next year's team a master student in drives and power electronics could look into details about building a custom motor controller.

Motor parameters

To find the best design the criteria used was 5 Nm and 270rpm. This should be the operating point for the motor when the car was cruising at a steady 28km/h. However these values are not critical because the design which is the most efficient at this operating point would also be the most efficient at other operating points since all possibilities considered here is the same type of motor, just different geometries. That means they'll behave the same.

To identify the most efficient design Maxwell 3D was used to simulate the flux linkage and thereby induced voltage. This number was then used in a series of equations to estimate the performance of the machine.

The loading of this machine is low and since there is no iron in rotor or stator it is assumed to be completely linear.

Table 1: Design parameters of the chosen geometry.

T [Nm]	5,000
P_{out} = 3*e*i = T*w [W]	141,4
I_f [|A]	3,282
ω = n/60*2*pi [rad/s]	28,274
e = (e/N)*n [V], rms	14,357
n [rpm]	270,0
e/N [V/rpm], rms	0,053
# pole pairs	24,0
# phases	3,000
# slots per pole per phase, q	1,000
Stw [mm]	8,700
D_o [mm]	320,0
D_i [mm]	210,0
k_D	0,656
Wire fill factor	0,550
Slot fill factor	0,455
Slot width, inner diameter [mm]	4,581
Slot width, outer diameter [mm]	6,981
Inner end turn length [mm]	30,0
Outer end turn length [mm]	40,0
Copper resistivity [siemens/mm], 60*C	50302,4
Copper area [mm^2]	10,961
Wire length per phase [mm]	8160,0
Phase resistivity [ohm}	0,015
Copper loss [W]	0,478
Eddy current losses [W]	0,050
Mechanical losses [W]	2,820
Efficiency [%]	97,700
Efficiency without mechanical loss [%]	99,628

3D model in Maxwell

To ensure proper simulation results 3D modeling was chosen as the primary tool. Figure 2 shows the model in Maxwell.

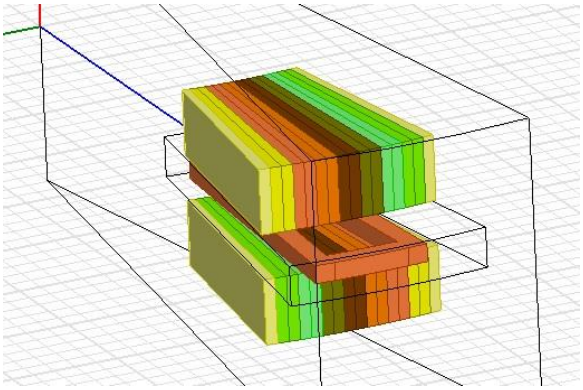

Figure 2: 3D model from Maxwell showing one pole pair.

Figure 3 shows the mesh used in the simulation. Many nodes were needed in the air gap to give accurate simulation results.

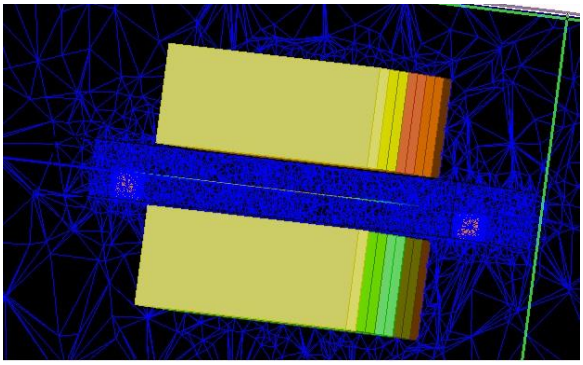

Figure 3: Air gap mesh.

Transient solution was used to calculate induced voltage in the winding. Figure 4 shows the graph with the peak value of the voltage marked.

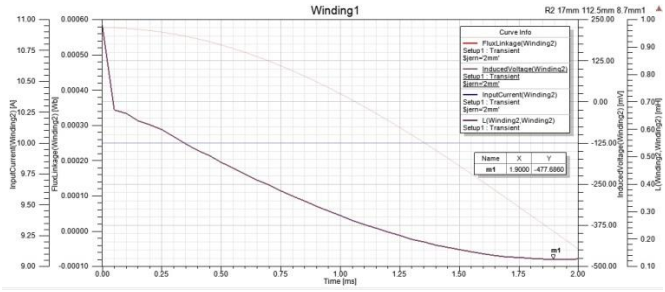

Figure 4: Induced voltage in the winding.

A model for how the weight affects the performance of the car has not been developed. Bigger magnets would mean a higher magnetic field and therefore a more efficient motor, but the extra weight would be negative for the performance. That means it was not easy to know how big the magnets should be. The old motor weighted 21kg including rim. With 10kg of magnets in the new motor the weight would be almost similar. Nasrin's design was lighter than this but with the track parameters and the knowledge about the winning car from last year the belief was that weight is secondary.

The decision was made to go with 10kg of magnets and end up with a very powerful motor and a weight similar to the old motor. Simulations were done to find the best use of these 10kg and the results are showed in appendix A1.

Varying air gap was tried, but even though the simulations were promising the idea of a thinner stator was abandoned because an error in the stator production would be more severe.

Figure 4 shows the induced voltage calculated by Maxwell. This was checked by running a magneto static analysis, finding the maximum average B-field in the windings and then calculating the amplitude of the induced voltage by the formula below (Hanselmann, 1993).

$$e = \frac{d\lambda}{dt} = 24 * 2 * \frac{\lambda_{max} - \lambda_{min}}{\Delta t} \quad (1)$$

With 270rpm the time to move from one pole to another is 0.0046s. So Δt is 0.0023s. λ_{max} is the area of the coil times average B-field and λ_{min} is zero.

The area of one coil is 0.000954m^2.

The average B-field was found looking at the variation of the field along three lines in the air gap, shown in the contour plot in figure 5. The center point where the lines meet is in the middle of the air gap.

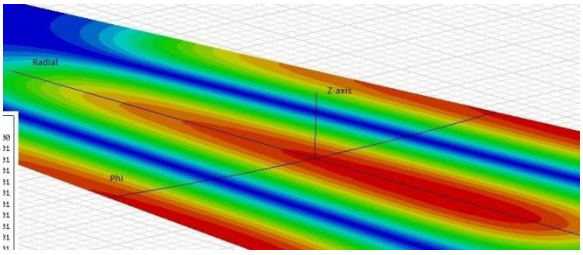

Figure 5: Contour plot with lines.

The following figures show the distribution of the B-field along these lines. In the center point the field strength is 0.96T.

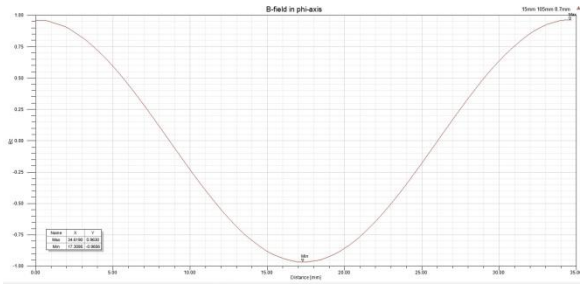

Figure 6: B-field distribution in phi-axis.

In the phi-axis the field is sinusoidal as shown in figure 6. The average value of this is 0.644 times the peak value in the center point.

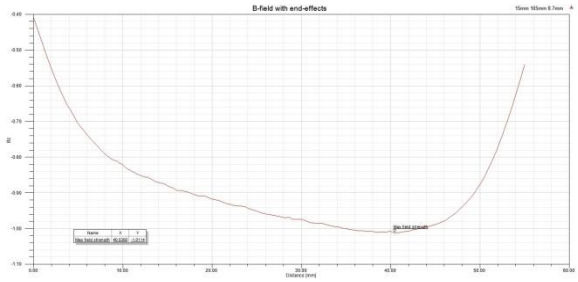

Figure 7: Radial B-field.

The average in the radial axis was calculated manually from the data table with all the points. The average was found to be 0.881 times the value in the center point. The distribution is shown in figure 7 and the data table is found in appendix A2.

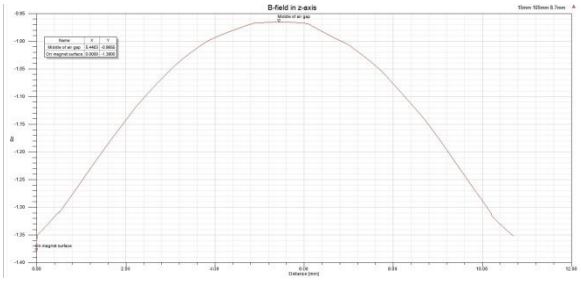

Figure 8: Axial direction B-field.

In the z-axis the field is symmetric as shown in figure 8, and the average value was calculated to be 1.111 times the value in the center point.

Then the average B-field is estimated to be

$$B_{avg} = 0.644 \times 0.881 \times 1.111 \times 0.96 = 0.61T$$

And the induced voltage

$$\mathrm{e} = \frac{d\lambda}{dt} = 24 * 2 * \frac{0.000954 * 0.61}{0.0023} = 12.15V$$

This gives an rms value of 8.87V compared to the value from Maxwell of 14.36V it's a lot lower.

Another thing was tried. The line spanning the radial direction was moved to the point where the field was equal to the average value in both

phi-axis and z-axis. It was moved 1.6 degrees in phi-direction and 3.15mm in the z-direction. Then the average B-field along the line was calculated to be 0.735T. Using this value the back induced voltage becomes 10.69V. Still lower than what Maxwell calculates, but it looks like that the variation in phi-axis is lower when the line is moved out from the center.

With the test results later in the report in mind and the fact that production was not perfect it is assumed that the values that Maxwell calculates are the correct values.

Magnet forces

The magnets on the two rotor plates will try to close the air gap. Bearings, rotor plates and the glue to hold the magnets have to be dimensioned for this force.

This force can be estimated by the following formula (Endresen, 2012):

$$F = \frac{B^2 \times A}{2 \times \mu_0} \qquad (2)$$

With the average field strength 0.735T calculated earlier and the total area of 0.0458m^2 the force becomes 9.8kN in total.

This was also simulated in Maxwell to be 316N per pole pair as shown in figure 9 and thereby 7.6kN total force. This value was used when the thickness of the aluminum plates for the rotors was chosen.

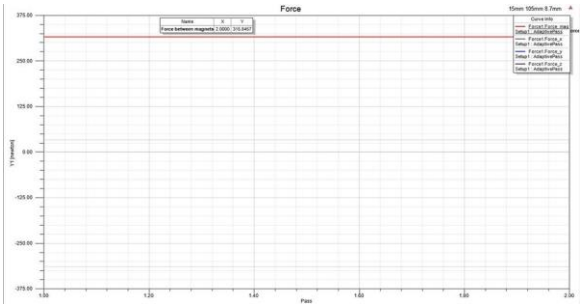

Figure 9: Magnetic force between two poles.

Magnetic loading

High grade magnets have a non-linear magnetization curve. Too high loading will demagnetize them, but even if they are not destroyed the performance is low if they operate outside the best operating point.

The magnetization curve for the NdFeB N52 magnets is shown in Appendix A3.

The magnetic loading can be calculated from the formula below (Hanselmann, 1993). This value is thought of as the slope of a line going from origin and crossing the demagnetization curve.

$$P_c = \frac{l_m \times A_g}{g \times A_m} \qquad (3)$$

Finding the equivalent values for area and length of the magnet in a Halbach array is not the easiest task, but an approximation is to just use the length of a half circle through the magnets to find the length and use the surface area of one pole as the equivalent area. This is shown in figure 10 and table 2 on the next page.

We see that longer magnets and wider air gap gives a higher P_c while a longer air gap and wider magnets gives a lower P_c. Here the width of the air gap is assumed to be the same as the magnets, but in real life this would not be the case. This would lead to a lower operating point.

With the equivalent values at the middle radius given in table below the permeance coefficient becomes 1.9. The load line is plotted in figure 11.

This estimate shows that the magnet array should operate above the knee of the curve and not loose performance.

Table 2: Equivalent values of Halbach array.

Parameter	Equivalent Value
l_m	20.4mm
A_g	357.5mm^2
g	10.7mm
A_m	357.5mm^2
P_c	1.9

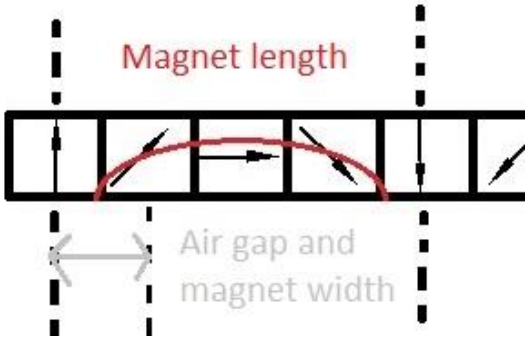

Figure 10: Equivalent geometry of Halbach.

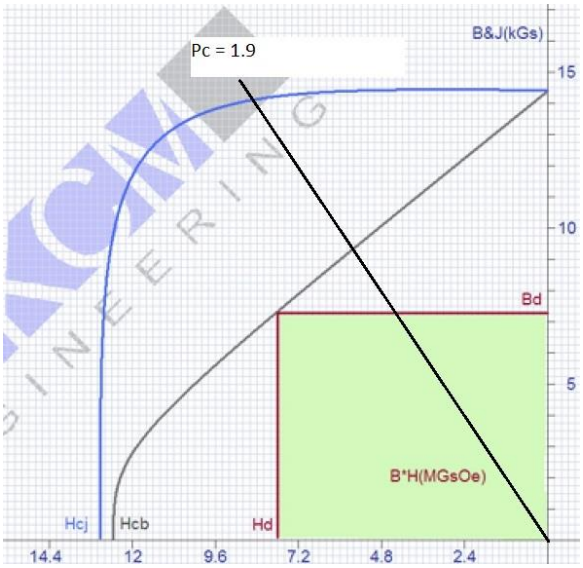

Figure 11: Demagnetization curve with load line.

Stator

The two most promising methods for stator design were Litz wire and solid conductors water cut from a copper plate.

Litz wires have been used earlier to prevent losses because of eddy currents and proximity effect. This is based on the skin depth, which basically means the current do not flow in the center of the conductor at high frequencies. This leads to higher losses because the copper is badly utilized. These wires are used in many high frequency applications. Litz wires work because there are many thin strands which is insulated from each other and then twisted. This gives a uniform current distribution and eddy currents are heavily damped.

The water cut windings would have a much better fill factor than the Litz wire, which would reduce the copper losses. The fill factor in the slots could almost be doubled with regards to Nasrin's design with Litz wire because the area doesn't need to be constant and there is almost no insulation. The drawback of this design is the eddy currents.

To estimate the eddy current loss the equation below (Hanselmann, 1993) can be used.

$$P_{EC} = \frac{1}{12} \times \sigma \times l \times stw \times w^3 \times \omega^2 \times B^2 \quad (4)$$

This number can then be estimated for Nasrin's design with a total of 144 slots. For one solid conductor in the slot this loss equals 22.3W per slot and thus 3222W for the whole machine at the rated speed of 25km/h. This loss is not dependent on the loading of the machine, but the speed. To achieve the right back EMF in Nasrin's design four turns are needed. If the width are divided into four series connected conductors the eddy current loss are reduced to 189W. This was verified in Maxwell 3D and later a water cut winding was made and tested in the lab by a fellow student to give the same result [8].

Due to the calculation and simulation results it was decided to use Litz wire. With the super strong permanent magnets the induced voltage per turn was very high. Therefore it was decided to only have two turns. In addition it was initially a thought that this would lead to an easier production process.

The wire used was custom made by New England wire technology in the USA. The specification was Type 2 Litz 7 AWG 7X30/30 SPN. This means it has a copper area equal to a 7 AWG, which is the same as 10.5mm^2. It is made up by 7 twisted strands which again are made up by 30 twisted 30 AWG wires. That means it is 210 strands twisted in two levels.

This was pressed into a rectangular wire with the dimensions 4.3mmx4.5mm to accurately fit into the slots in the machine.

The fill factor of this wire is then 55.2% and the slot fill factor would then equal 45.6%.

Epoxy was used to give the winding mechanical integrity and a way of mounting it to the axle. This was bought from Lindberg & Lund. 17110 Araldite DBF together with the hardener HY956B 11796 Ren HY956 MP was used because of the relatively easy handling. It would not be necessary with vacuum or hardening at temperatures above room temperature.

Wave winding arrangement was used due to the short end turn length compared to the active length of the winding and therefore the quite efficient design. Figure 5 shows the winding before its being casted in epoxy.

The windings were done in such a way that they could be laid down phase by phase in the mold. This meant the end turns of the different phases did not cross each other and this can be seen in figure 12.

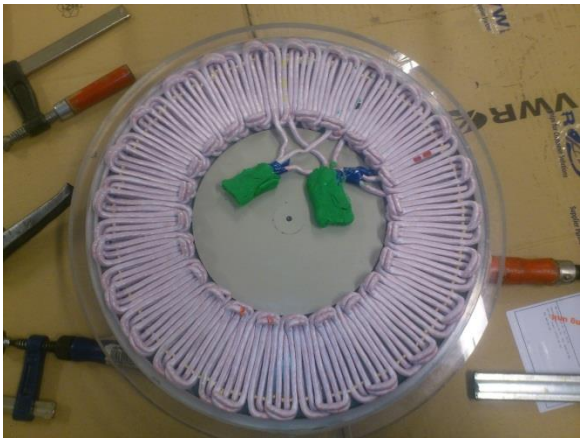

Figure 12: Wave winding.

Figure 13: The end turns of the top phase is always crossing on top.

In figure 13 a paper with all holes marked can be seen. This was used as a guideline so the wires would not crash with any of them after the stator was casted in epoxy.

The mold was made in Polystone which is a quite stiff plastic material. A small prototype of the stator was first made to see if this worked at all. This mold was made as a two-piece design and not for vacuum casting. Details of this work can be seen in figure 14 to 17.

A wooden plate was also machined with slots so one winding at a time could be made. When one phase was finished it was moved over to the mold and the next phase was made. This is seen in figure 8 and 9.

Figure 14: Prototype stator mold.

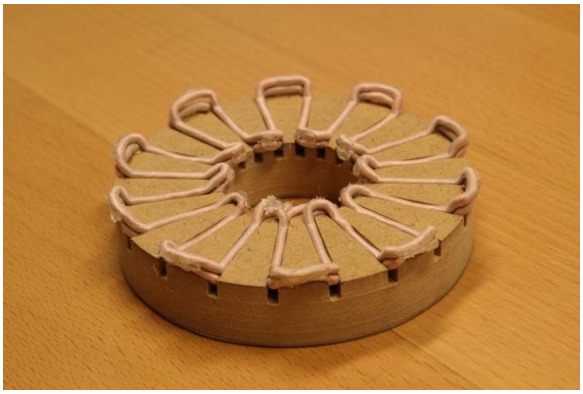

Figure 15: The top phase is finished and ready for the mold.

Figure 16: The complete three-phase winding is ready to be casted in epoxy.

Figure 17: Prototype stator finished.

Figure 17 shows the final result of the work with the prototype. It was a success and it was decided to use the same technique for the real stator.

A problem was discovered when the big stator mold was to be made. The bottom part was supposed to be machined down in a CNC mill. This was not possible to do because of internal stress in the plate that basically bent the whole plate. Therefore a three-piece mold was made. This solved the problem because the slots for the end turns and a spacer ring at the outside were the only machining necessary. Figure 18 shows the final mold. The spacer ring was machined from a Lexan plate and was 8.7mm thick.

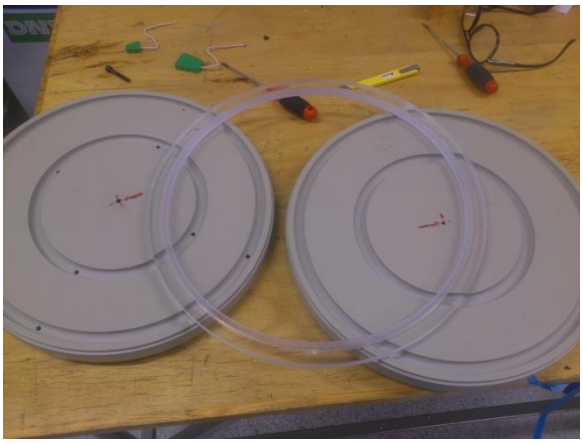

Figure 18: Final mold for casting the stator.

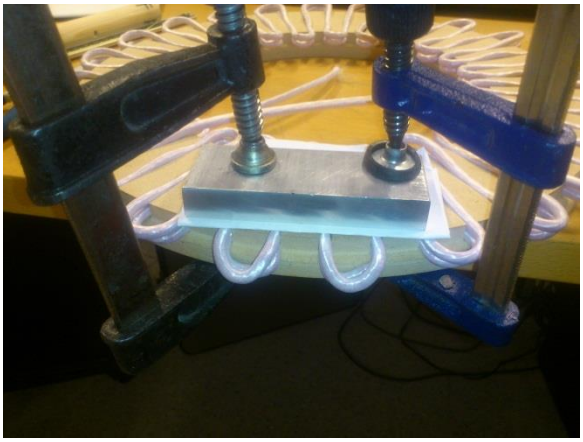

Figure 19: Bending of the end turns.

Because of the stiffer Litz wire for the real stator tools had to be used to bend the end turns. This can be seen in figure 19. Care had to be taken not to damage the wires in the process.

When the windings was placed in the mold it had to be pressed together to ensure it wouldn't be too thick. The hydraulic press was used for this to put the wires in the right place. During casting powerful clamps was used as figure 20 shows.

Bits of fire sticks were used between the wires to ensure even displacement between them.

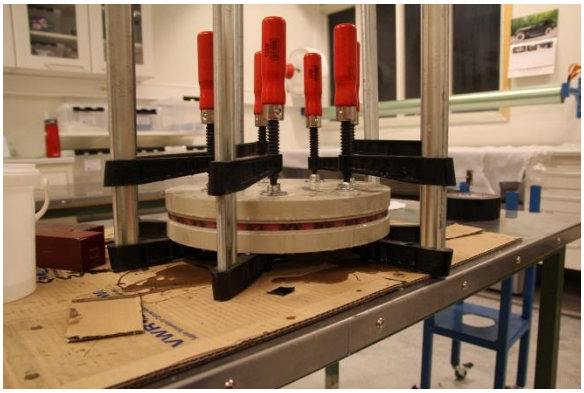

Figure 20: Epoxy casting.

The final result can be seen in figure 21 and 22. The thickness should be 8.7mm, but was found to vary a bit, and was 9mm at the thickest point.

But with 1mm air gap at each side this was no thought of as a major problem.

There are mainly two reasons for this. The most important one is that the windings were a bit too tight at the inner diameter. From the start the goal was to put as much copper in there as possible. Therefore the slot width at the inner diameter was used as a parameter and the winding is just a bit smaller than this value. What should have been used is the slot width inside of the inner end turns. This would have provided more space at the inner diameter. A steel mold would however solve this problem because it would not bend as much as the Polystone mold. In the future a steel mold should be made anyway to ensure that everything is in place. Another thing that's important with the stator mold is slip angle. The mold used didn't have enough slip angles, so it was very hard to get the cast out of the mold. Air at high pressure was blown into the center holes, but this wasn't enough

Figure 21: Finished stator.

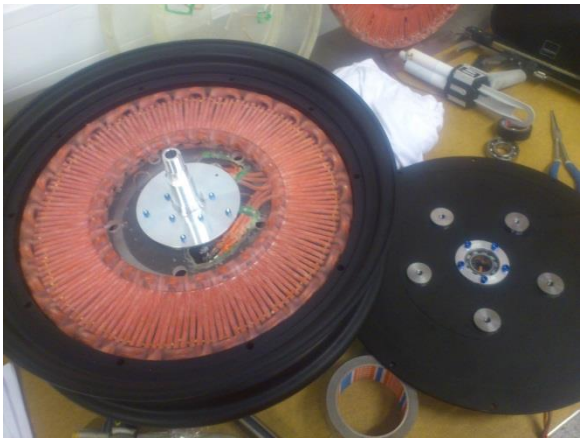

Figure 22: Stator mounted on the axle and placed inside the wheel.

The resistance in the windings was measured after the stator was finished to ensure that everything still worked. The result is shown in table 3. Since the exact length of wire in each phase was not measured the theoretical value is not known, but 9.5m of 10.5mm^2 copper wire should have a resistance of 15.8mΩ. The middle winding was shorter than the lower and upper winding so that's why it has a lower resistance.

Table 3: Resistance of phase windings.

Winding	Resistance mΩ
A	16.3
B	15.8
C	16.2

When looking at the stator it can be seen that it is not perfect. The wires do not lie in a completely straight line or completely axially. This lowers the induced voltage as the winding factor gets lower. Since the number of poles is so high the number of electrical degrees the windings is skewed gets quite high quite fast with small errors in production.

Rotors

The motor should have a double rotor with permanent magnet configuration. Nasrin proposed to use Halbach arrays because of the higher flux density compare to a conventional north south configuration [1] and [9].

Endresen put together a pair of nice rotors with 90° N42 Halbach array. After simulations in Maxwell it was found that a 45° array would increase the back induced voltage by 9.8% compared to a 90° array of the same size and magnet grade. This is similar with the findings in [10]. Figure 23 shows a 90° array and figure 24 shows a 45° array. The magnets in the 45° array would be half the size, and twice as many would be needed.

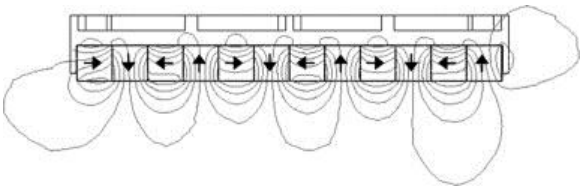

Figure 23: 90 degree Halbach.

Figure 24: 45 degree Halbach.

Drawbacks with the 45° array are more complicated assembly and the higher material cost. The cost was not really an issue because of the proper funding of the project and the motor development. The assembly should however be an important part of the process to get the motor finished before the race.

A 45° array of NdFeB N52 magnets was ordered from Ningbo Xinfeng Magnet Industry Co.,ltd in China. They would have a B_r of 1.43T and was one of the most powerful magnet grades available.

Figure 25 shows the field strength in the middle of the air gap with this magnet array simulated in Maxwell. The powerful magnets did push 1T through the conductors.

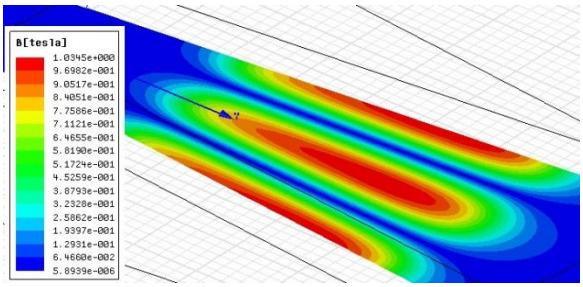

Figure 25: B-field in the middle of the air gap.

Assembly of the magnet array proved to be more challenging than anticipated. In figure 24 it can be seen that there are especially three magnets per pole that are not very good friends. There is one pointing directly up and the two neighbors of this magnet do also point up, but in a 45° angle. These three had to be forced together if the array was to be stable. With two rings this meant that 96 of these groups had to be glued together before the final array could be assembled.

This work wouldn't have been so hard if the magnets had arrived in time. But because of problems with placing the order, holidays and manufacturing process the magnets arrived very late. So late that several team members had to work almost nonstop from the day the magnets arrived and until the rotor plates were glued and done if the new motor was to be finished before the race.

The magnets were ordered on 5th of February, but arrived in Trondheim on 3th of May. The car was supposed to leave for Rotterdam on 11th of May, just over one week later.

To be able to assemble the three difficult magnets tools had to be made. The initial

thought was that steel was not a good idea since it's magnetic. A mold with two slots was designed. The slots were wide enough for two and three magnets to fit, respectively. This way two magnets could be glued together first and then the third could be added. This was milled in a piece of aluminum in the Makino CNC mill.

Figure 26 to 28 shows this first mold. Figure 28 show the top part as well that should keep the magnets flat while there was screws on the side that pressed them together.

Figure 26: CNC machining.

Figure 27: Mold to glue magnets together.

Figure 28: Finished with a powerful top part to hold the magnets in place.

This first mold did not work. The magnets did not want to stay in the slots and there was too much pressure for the glue to work properly. This mold could however not be made in steel because it would be almost impossible to get the magnets out of the slots after gluing.

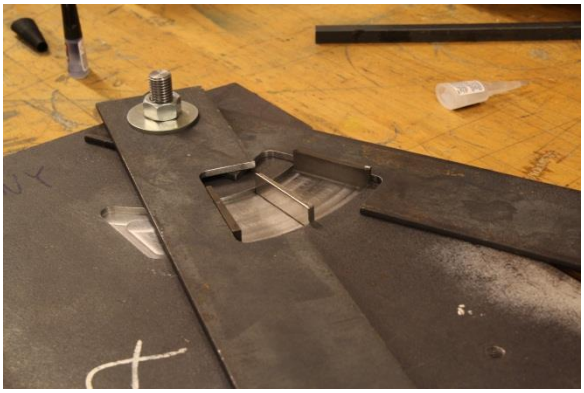

Figure 29: Jig for assembling magnets.

Therefore new tools had to be designed. Figure 29 shows a jig that was made to be able to put together the magnets. A slot was milled in a steel plate where the magnets just fitted into. The jig had these two arms that pushed the magnets together and a rod was put on top to hold them down to the plate. This process can be seen in figure 30. Steel was chosen because that was the only way the magnets wanted to

stay together long enough for the glue to do its magic.

Figure 30: Steel in all directions was the only way to keep the magnets in place.

When this was done the array could be put together. Figure 31 shows the progression. The ring on top is aluminum. The glue used between the magnets and the rotor plates was AW4858-HW4858-SP from Lindberg & Lund.

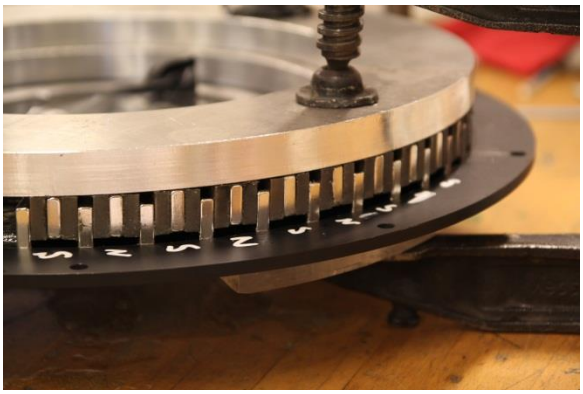

Figure 31: Halbach in the making.

Figure 32 and 33 shows the final rotor rings. There were some problems with the magnet rings. The jig that was used to put the three magnets together was made in a hurry and it didn't glue the magnets completely true. This meant that the magnets didn't quite fit into the slots that were already machined in the rotor plates. The rotor plates and the rim were machined for free at a local company called Delproduct AS as a part of a sponsorship deal with the DNV Fuel Fighter team.

This leads to several problems. The side facing the stator was uneven and the 1mm air gap was not enough space. The side facing the plate was also uneven and the glue didn't get to work that well. Some magnets came loose and had to be glued again.

The most serious problem was that the magnets was skewed a bit and that meant the last magnet in the array didn't fit. So it had to be replaced with a steel piece instead.

Machining of the magnet was tried, but it got too hot and was thereby destroyed.

Figure 32: Gluing finished.

Figure 33: Finished rotor plate with magnets.

A simulation was done with 1.5mm air gap on each side and the induced voltage decreased by

6.4%. The exact value for the air gap in the motor is not known, but it's closer to 2mm on each side after spacing because it was difficult to find thinner spacers and at the same time have enough room for the stator.

Also on the side, in the radial direction, the design had a 1mm gap between stator and the magnets. This was a mistake. Because of the uneven magnet array the stator touched in this direction as well and the corners of the magnets had to be grinded down. This value is not critical for the performance in any way and should have been made at least 2mm to ensure enough space.

The team wanted to finish the new motor badly due to all the new mechanical parts associated with it. The new aluminum rims were completely true, easier to handle than the old carbon fiber rims and could withstand the air pressure in the tires of 5 bars with no problems.

Losses

The different losses are estimated by analytical calculations. Copper loss is calculated from the needed phase current and the resistivity in the winding which again is a result of copper area and wire length.

$$P_{Cu} = 3 \times R_a \times I^2 \quad (5)$$

In this design this loss at 5Nm is 0,535W.

The Litz wire that was used had 210 strand each with a diameter of 0.255mm. With 2 turns, 3 phases and 48 poles the eddy current loss at 270rpm with a flux density of 1T becomes 0.051W when using equation 4.

The friction and windage losses are calculated from the following equations [11] and [1]

$$P_{Fr} = F_{load} \times k_f \times d_{bearing} \times \omega \quad (6)$$

$$P_w = \frac{1}{1} \times c_f \times \rho \times (2\pi n)^3 \left({R_{out}}^5 - {R_{in}}^5\right) \quad (7)$$

The friction loss is estimated to be 2.80W with a load of 120N, weight of rotors, k_f equal to 0.01 and equivalent diameter of 25mm for the SKF hybrid ceramic bearings. Windage loss was estimated to be 0.023W so the total mechanical loss is then 2.82W.

This is higher than the value first estimated in Nasrin's thesis, but should be more accurate since it's the model of the bearings that are used in the motor. This means that the friction loss used in the analysis is too low. All the values in the appendix use the value 1.6W which is what Lubna calculated. The theoretical efficiency of the design used here is reduced from 98.43% to 97.70% due to this.

Encoder

Previous years the motor has been run by a sensor less algorithm. This is not an ideal way of operating a synchronous motor. To get maximum torque of a given current in the stator windings the angle between the field in the rotor and stator should be as close to 90° as possible. This cannot be done if the controller can adjust the voltage vectors quickly if the angle passes 90° - it would lose synchronism.

Therefore it was decided to use an optical encoder with the motor. To find a suitable encoder was challenging. In this axial flux motor the axle is standing still and most encoders out there was supposed to fit on the axle. Therefore a different solution had to be made. What the team ended up with was to buy loose parts from US Digital in the USA. The EM1 read head together with the 2” disc and proper hardware to make this fit to the motor controller, like differential board and proper cables were ordered. Figure 34 shows the modified old motor and figure 35 shows the new motor with encoder installed.

Discs with 2500 slots were ordered. This was a mistake as the motor control software would have liked a proper computer number, i.e. 2048 much better. The reason for this is that the controller needed to divide this number and 2500 did not give an even number which lead to miscalculations. Help from Smart Motor to identify this and rewrite the software did solve this problem in the end.

With limited space inside the motor it was decided to have the encoder disc on the outside. A plastic cover was made to protect the disc. The hole in the axle was made big enough for the cable to go through and into the car.

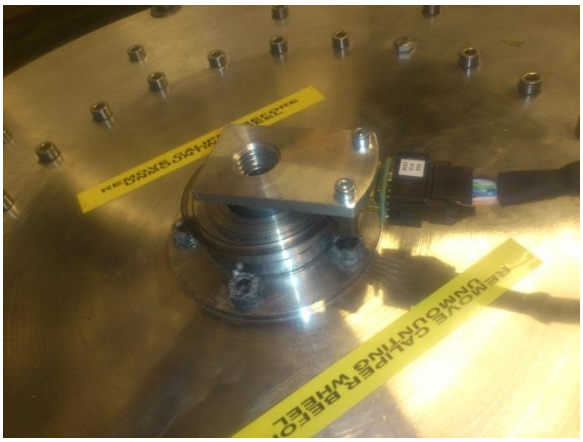

Figure 34: The old motor was also modified to work with encoder.

Figure 35: The new motor with encoder fitted and cable going through the axle.

Testing

To verify the performance of the final result the motor was setup in a test rig. A DC motor was mounted as load and a torque transducer was used to measure output power. A Harmonics analyzer was used to measure power going into the motor from the motor controller and a DC power meter measured the power going into the motor controller. In addition an oscilloscope was used to check voltages and output values from the equipment. The test setup is showed in figure 36.

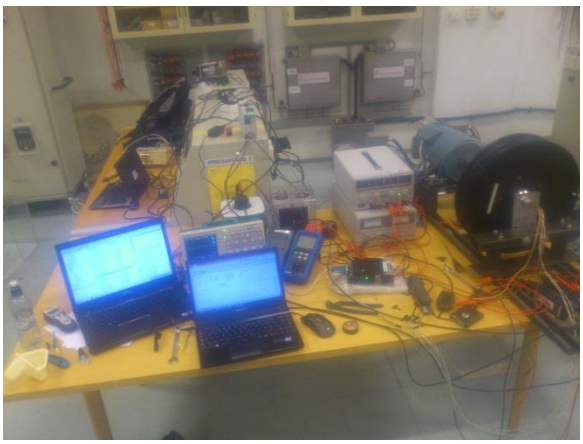

Figure 36: Test setup.

The following tests were performed:

- Dummy stator test
- No load test with real stator
- Performance test

This way the hope was to identify the different losses in the motor. When running with the dummy stator only the mechanical losses are present. This is useful when doing the no load test with the real stator because if the mechanical losses are subtracted from that result what's left is the eddy current loss.

Results

All results that are based on the output torque have to be used with caution. Because of the placement of the encoder on the outside of the rotor plate there wasn't really possible to fit the adapter for the torque sensor in a good way. A vacuum formed plastic cup was placed outside of the encoder and holes were drilled in the plastic to be able to fit the torque adapter. This solution wasn't very good because the two motors have to be mounted very accurate. A flex coupling was used on the axial flux motor, but it could be seen when the motor was running that the adapter was not in line with the test setup.

Figure 37 shows the mechanical losses. This is friction and windage loss. At 270rpm this loss was measured to be 6.4W which is 227% of the calculated loss of 2.82W.

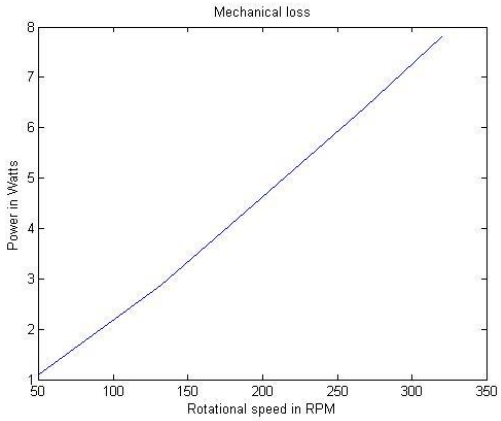

Figure 37: Mechanical loss as function of rotational speed.

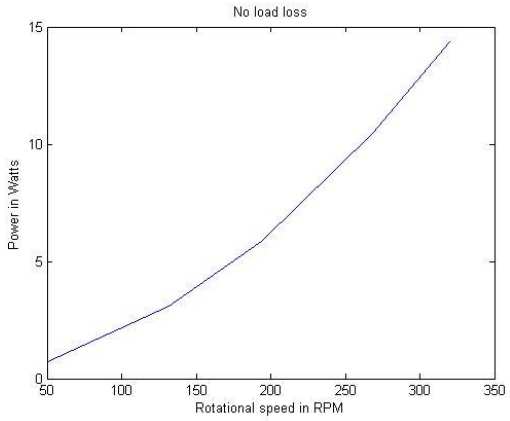

Figure 38: No load rotational losses.

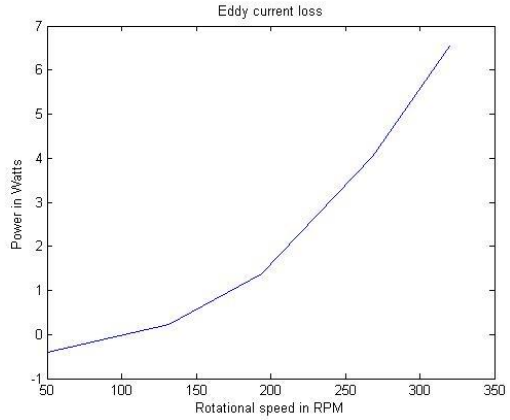

Figure 39: Calculated eddy current losses.

Figure 38 shows the total rotational losses. At 270rpm this loss was measured to be 10.4W. If the friction loss is subtracted from this value the remaining is assumed to be the eddy current loss in the stator windings, this is showed in figure 39. The theoretical eddy current loss was 0.051W whilst the calculated loss in this case is 4.04W. That is 79 times as much.

The back induced voltage was measured. Since this is a pure voltage measurement and was measured with an oscilloscope this is probably the most accurate test. The voltage waveforms are shown in figure 40 and the voltage amplitude as a function of rotational speed is shown in figure 41.

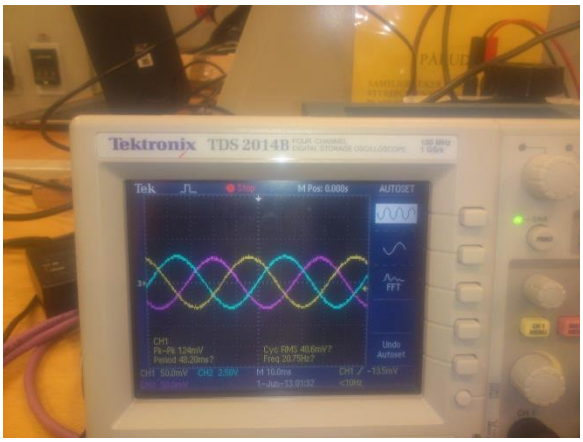

Figure 40: Oscilloscope was used to verify the three phase voltages.

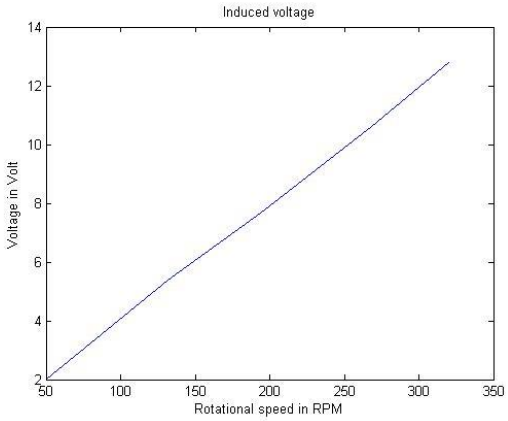

Figure 41: Induced voltage as function of rotational speed.

Here it can be seen that at 270rpm the back induced voltage is 10.6V rms. The theoretical value was 14.3V and this difference is the errors from production. That is a difference of 35%. An interesting thing to do is to put this voltage into the equations in table 1. Then the result is still an efficiency of 99.0% if all rotational losses are discarded.

The last test was running the motor with load. The large rotational losses ruined the efficiency, but it was still measured to 96.3% at 275rpm and 5.2Nm. Figure 42 shows the results, the lower curve includes rotational losses while the upper is without. When subtracting the

rotational losses measured earlier the efficiency is calculated to 100.7% so the number looks to be a bit optimistic. And the fact that at 310rpm and 4.75Nm the efficiency is down to 87% clearly shows that the measurements are not conclusive.

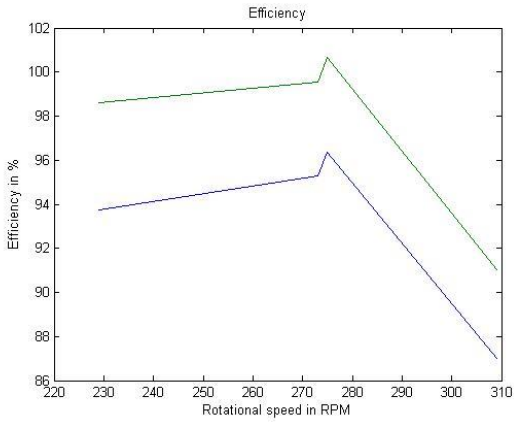

Figure 42: Efficiency of the motor.

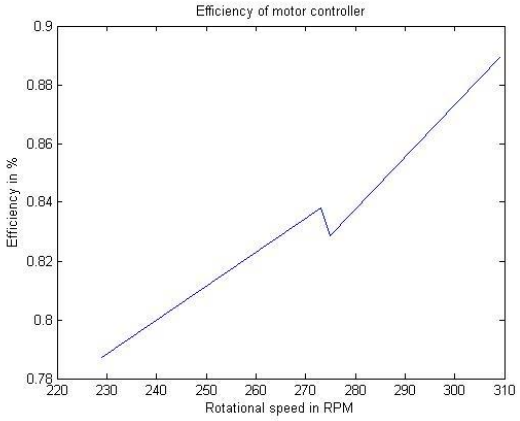

Figure 43: Efficiency of the motor controller.

Figure 43 shows the efficiency of the modified motor controller from Smart Motor. It varies from 78.7% at 230rpm and 4.34Nm to 88.9% at 310rpm and 4.75Nm. This shows that the controller is more efficient at higher loads.

Batteries

A123 Lithium Ion batteries with a nominal voltage of 46.2V and in three different sizes were provided by Gylling Teknikk. Last year's team thought the batteries could not provide enough power without having too much voltage drop.

The medium and the large battery were tested with a variable resistor with 15A load current. The medium battery had initially a voltage of 46.64V. With 15A current drawn from the battery the voltage went down to 43.35V.

The big battery had initially a voltage of 46.78V. With 15A current drawn from the battery the voltage went down to 44.5V.

So this proves the batteries should be able to keep the voltage quite stiff even if the motor controller draws 650W.

The batteries had built in automatic BMS. However this did not include thermal cut off which had to be in place to meet the 2013 regulations. This was solved by soldering a thermal fuse in series with the battery management system and placing it just at the end of the battery. The thermal fuse would melt at 72°C.

Motor controller

The motor controller that was used was provided by Smart Motor. It a controller originally built for use in a submarine, the Hugin. Earlier years the team did not have much control of the digital signal processor software. This has led to problems because every time a change had to be made it had to go through Smart Motor.

Therefore some effort from the guys working at Smart Motor was put into making a software package that could be used by the students and giving the team control of everything necessary. This worked out very well and the code was quite understandable as it did hide most of the lower layers in the code and at the same time provide a control of all needed parameters in a structured way.

The controller hardware had to be modified to work with the encoder since earlier teams had run a senseless algorithm and the encoder card was not installed in the motor controller. The cooler had to be cut to make space for the extra circuit board. At the same time high performance cooling paste and aluminum screws was installed.

Because this controller is made for a submarine it has more functionality than this project requires. A quite high no load loss of almost 10W was measured for the controller alone. After investigating where the heat was produced and discussing with Smart Motor it was decided to remove the integrated circuits and mosfets originally used to control the rudders. As it turned out these circuits was active anyway and did draw some power. Approximately 2W was saved by doing this.

To ensure an efficient way of driving the motor a lot of time went into tuning the current regulators. Because the inductance of this ironless machine is very low there is not much filtering at the output of the controller and therefore difficult to produce a stable sine wave. By using a debugger program called Active DSP and using the scope function there to see the current wave form the best parameters for the built in PI-regulator was found. To begin with the motor produced a lot of noise, inverter noise because of vibrations in the stator due to the sudden current spikes.

To make it perfect was impossible so an idea was to try adding small inductances in series with the motor to increase the filtering capabilities. There would be some loss in the inductances, but it the thought was that the system would be more efficient. Looking at the Csiro motor again, it can be seen that this motor is delivered with a set of inductances.

Sadly due to time constraints and difficulties with the electric system right before the competition this test had to be abandoned.

The competition

As already mentioned the week before the race was very stressful. The electronic system did not work properly and the car did not pass the technical inspection. A faulty signal cable was found eventually after trying to replace almost everything. Then the car worked brilliantly, but all optimization of the car had to be abandoned due to this. Only one attempt was completed, on the last day, which led to third place in the competition. The team thinks this could be improved by just optimizing the software, driving controls and tactics in general. The car crossing the finish line can be seen in figure 44.

After the race we spoke to a French guy who earlier had been participating for the French team which won the competition and now was working as a marshal during the event. He meant the car should be ready two months before the competition so that everything could be tested properly and optimized. In the battery electric class the software and driving strategy is quite important since no time is needed to make the power source, the battery, to work properly.

The conclusion was that our car looks really good, and most likely the car itself was one of the most high tech at the event, but we didn't win because we didn't have the proper control software and driving strategy.

Figure 44: Crossing the finish line.

Figure 45: At display in DNV's main office in Oslo.

Still we managed to get two prizes - the design award and the PR award. So even if we didn't manage to do everything that we wanted and what it takes to win the battery electric class the project was a success with the third place on track and two off track awards. After the race the car and awards was on display at DNV, the projects most important sponsor, in Oslo, shown in figure 45.

Conclusions

Building a new motor was successful in the end. The motor was used in the competition and performed well. The building did not go without problems and the most severe ones were due to time restrictions. If the magnet had arrived on time the team could have spent more time building a revised jig and managed to glue them completely true.

Most effort went into building the stator as this part was thought of as the most difficult to produce from the start. This production method worked very well, and with some revised parameters for the Litz wire and a stiffer mold it could be perfect. The stator used in the motor is not very bad, but together with the irregularities in the magnet arrangements the air gap had to be made bigger to make sure the stator did not scratch the magnets.

The tests performed on the motor are not conclusive. The measure rotational losses are a lot higher than anticipated. Together with the knowledge about the adapter used for the torque transducer and the difficulties aligning the motor in the test bench the results have to be treated carefully. The test of the induced voltage does however indicate a fairly high performance. This test does show the flux linkage and the error of 35% can be the production errors.

The flux linkage would be lower due to some irregularities in the stator windings, the skewed and a bit broken magnets and the increased air gap. There is no reason to believe that if the production went completely smooth the induced voltage would be lower than in the design.

The high rotational losses have to be investigated more. The bearings could have more friction due to the axial loads the magnets produce, but also the eddy current losses are a lot higher than anticipated.

Future work

Firstly it's important to repeat the words from the French guy who has been on the winning team. The car should be finished a long time before the competition so the team has time to optimize everything. In the battery electric class the driving strategy and control software is one of the most important parts for a good result.

This motor could be tested again with a revised torque adapter. To identify the magnitude of the friction and eddy current losses would be important to know what to do with the next design.

A complete car model should be made and analyzed. This way the next team could get better understanding of the weight penalty compared to raw efficiency in the motor. This way a better optimization algorithm can be developed.

To completely understand the sereneness of the eddy current losses a FE-model should be made. This has not been done so far because of problems with the mesh in the air gap when the wires become so thin, but a method of making this should be investigated. PhD. Candidate Zhaoqiang Zhang can probably be of good help in this field.

To decrease system losses the motor could be designed with a bit higher induced voltage. The low voltage and high current stator produced here would lead to higher copper losses in cables, connections and controller. With the stiff battery voltage the induced voltage in the motor could be a bit higher.

Development of a new motor controller is the next step. It could be done by the help from Smart Motor and a master student in the field of power electronics and drives. An efficiency of more than 90% should be possible.

For a new motor development for 2014 a new stator mold should be made. Epoxy casting works well. The mold should be made in steel, this is possible to machine in the Makino CNC mill, to ensure a completely stiff mold. The size of the Litz wire should be revised to ensure there is enough space at the inner diameter. To use the hydraulic press a bit is good, but not as much as we needed to do. Finding a way of making the windings completely true would be a good improvement. This is especially for a high pole machine like this where the winding factor is easily affected.

A Litz wire with thinner strands should be used if calculations or simulations show that this could decrease the eddy current losses measured in this motor and the measurements are trustworthy.

New magnets should be bought. Halbach array should be considered again. If 45° array is to be used again it's important to consider the gluing process of the three problematic magnets. They need to be completely true and the glue would add a little bit to the width of the complete magnet array. Glue should be used between all the magnets. This way they could be glued together to a ring before gluing them onto the rotor plates. Then the slots guiding the magnets on the plates to ensure they are centered can be made accurately.

To make this simpler a 90° array can be used and the performance will not be that much lower. Especially if one anticipates that production of the 45° array might not go completely smooth.

Make sure to investigate holydays in China and production capabilities early when ordering high grade permanent magnets. Ideally the magnets should be ordered before Christmas so they would arrive in Norway in the first part of February. The same if a custom made Litz wire is to be used.

With a new rim or modifications to the old rim the outer diameter could be made even bigger because this design has room for M6 bolts going through the rotor plates and the rim to hold the wheel together. These screws are not needed as the magnets will hold the plates in place.

The last thing is the air gap in the radial direction that should be made bigger. 2mm here is nice comfort to be sure that if the stator touch it's in the axial direction. This would lead to a bit longer end winding, but the difference is very small compared to other losses.

Acknowledgements

I would like to thank my supervisor Professor Robert Nilssen for his support, guidelines and suggestions during this time period here at NTNU.

I would like to thank PhD. Candidate Zhaoqiang Zhang for his help and support about 3D modeling, especially Ansys Maxwell, and machine design in general.

The whole 2013 DNV Fuel Fighter team deserves huge thanks for letting me participate in this interesting project, and especially the two mechanical engineers Fredrik Pettersen and Magnus Holmefjord who has helped with the mechanical design of the motor and assembly.

Big thanks to the sponsors and supporters of the DNV Fuel Fighter project.

I would like to say thank you to my fellow students for a good time here at NTNU and suggestions for the work.

I would also like to thank my friends and family for supporting me during this work.

John Ola Buøy

June 2013

Trondheim, Norway

References

1 *Improved Version of Energy Efficient Motor for Shell Eco Marathon*, Lubna Nasrin Master Thesis 2011.

2 *Electric Motor Development for Shell Eco-Marathon*, Fredrik Vihovde Endresen, Master thesis, 2012.

3 *Design of an in-wheel motor for a solar-powered vehicle*, H.C.Lovatt, V.S. Ramsden and B.C. Mecrow, 1998.

4 Csiro, CSIRO Solar Car Surface Magnet Motor Kit, http://www.csiro.au/resources/pf11g.html

5 *Axial Flux Permanent Magnet Motor Csiro*. R. Al Zaher, 2010.

6 *A comparison between axial-flux and the radial-flux structures for PM synchronous motors.* Cavagnino, A., Lazzari, M., Profumo, F., Tenconi, A., 2001.

7 *Analysis and Performance of Axial Flux Permanent-Magnet Machine With Air-Cored Nonoverlapping Concentrated Stator Windings*, Maarten J. Kamper, *Member, IEEE*, Rong-Jie Wang, and Francois G. Rossouw, 2008.

8 *Analysis of a novel coil design for axial flux machines.* S. Lomheim, 2013.

9 *Improvement of Axial Flux Permanent Magnet Machine using Halbach Arrays*, Astrid Røkke , Project Work, 2006.

10 The Effect of Roll Angle on the Performance of Halbach Arrays
D. Maybury, C. Nanji, M. Scannell,; Magnetic Component Engineering, Inc.
F. Spada; University of California-San Diego, Center
for Magnetic Recording Research, 2008.

11 SKF, calculation of bearing friction. http://www.skf.com/group/products/bearings-units-housings/spherical-plain-bearings-bushings-rod-ends/general/friction/index.html

Appendixes

A1: Simulation results

The back induced voltage of the given geometry was calculated in Maxwell 3D. This value was then put into the equations and the efficiency at 5Nm and 270rpm was calculated.

Design	D_o [mm]	D_i [mm]	Stw [mm]	H_m [mm]	Halbach	Air gap [mm]	Back-emf [V]	Efficiency [%]
Old motor	315	205	6	10	No	2	0,31	95,823
Old motor	315	205	6	10	No	1	0,34	96,374
Lubna's design	315	247	8,7	8	90	1	0,233	97,638
New design	320	210	6,7	15	45	1	0,595	98,442
New design 2	320	210	7,7	15	45	1	0,554	98,44
New design 3	320	210	8,2	15	45	1	0,534	98,435
New design 4	**320**	**210**	**8,7**	**15**	**45**	**1**	**0,517**	**98,433**
New design 5	320	210	9,7	15	45	1	0,484	98,422
New design 6	320	210	8,7	17	45	1	0,528	98,451
New design 7	320	210	8,7	13	45	1	0,5	98,402
New design 8	320	150	8,7	11	45	1	0,598	98,273
New design 9	320	170	8,7	12	45	1	0,598	98,339
New design10	320	190	7,7	13	45	1	0,602	98,428
New design11	320	190	8,7	13	90	1	0,51	98,322
New design12	320	190	8,7	13	45	1	0,56	98,417
New design13	320	243	8,7	20	45	1	0,416	98,372
New design14	320	225	8,7	17	45	1	0,477	98,425
New design15	320	210	8,7	15	45	1,5	0,484	98,369

A2: Table of B-field values from Maxwell

	Distance [mm]	Bz Setup1 : LastAdaptive
1	0.000000	-0.406641
2	1.410256	-0.509787
3	2.820513	-0.601488
4	4.230769	-0.670286
5	5.641026	-0.724912
6	7.051282	-0.765327
7	8.461538	-0.799567
8	9.871795	-0.818558
9	11.282051	-0.842560
10	12.692308	-0.856203
11	14.102564	-0.871210
12	15.512821	-0.884530
13	16.923077	-0.895494
14	18.333333	-0.907180
15	19.743590	-0.914625
16	21.153846	-0.924993
17	22.564103	-0.935348
18	23.974359	-0.942071
19	25.384615	-0.954440
20	26.794872	-0.962279
21	28.205128	-0.969214
22	29.615385	-0.974267
23	31.025641	-0.983209
24	32.435897	-0.986016
25	33.846154	-0.993919
26	35.256410	-1.001340
27	36.666667	-1.006222
28	38.076923	-1.008418
29	39.487179	-1.009299
30	40.897436	-1.010822
31	42.307692	-1.004642
32	43.717949	-0.994766
33	45.128205	-0.987209
34	46.538462	-0.969556
35	47.948718	-0.939993
36	49.358974	-0.900336
37	50.769231	-0.840523
38	52.179487	-0.759112
39	53.589744	-0.658240
40	55.000000	-0.540286

A3: Demagnetization curve of NdFeB N52

HKCM ENGINEERING

Néodyme (NdFeB) N52

Update 12 June 2013

BH-diagram (de-magnetisation curve)

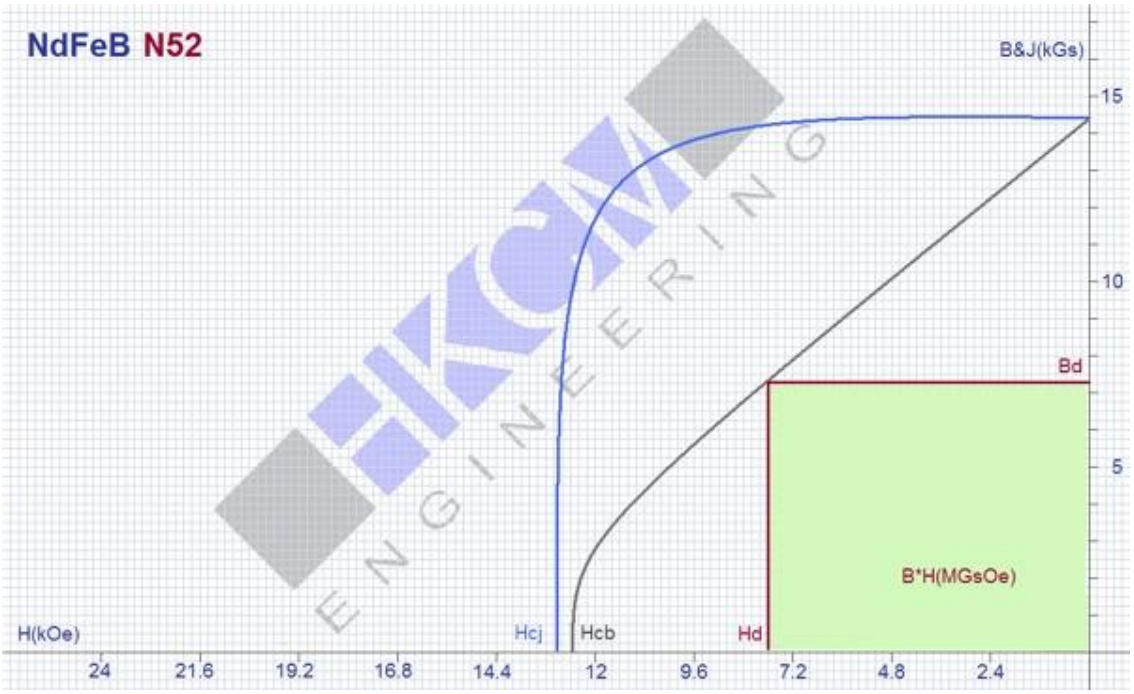

N35	PDF
N38	PDF
N40	PDF
N42	PDF
N45	PDF
N48	PDF
N50	PDF
N52	PDF
35M	PDF
38M	PDF
40M	PDF
42M	PDF
48M	PDF
50M	PDF
35H	PDF
38H	PDF
40H	PDF
42H	PDF
45H	PDF
48H	PDF
35SH	PDF
38SH	PDF
40SH	PDF
42SH	PDF
45SH	PDF
28UH	PDF
30UH	PDF
33UH	PDF
35UH	PDF
38UH	PDF
40UH	PDF

ENERGY PRODUCT = Hd*Bd = 52 Mega Gauss * Oersted (MGO)

Grade	N52	
Residual Induction Br	14.3-14.8 (1430-1480)	KG (mT)
Coercive Force Hcb	10.0 (796)	kOe(KA/m)
Intrinsic Coercive Force Hcj	11.0 (876)	kOe(KA/m)
Energy Product BHmax	50-53 (398-422)	MGO(KJ/m3)
Max. Operating Temp.	60	°C

For the description of the properties of magnets practical and theoretical comparisons need to be done. Magnetic materials preferably are conditioned and measured in electro magnetic fields.
The BH-diagram is used to determine a characteristical figure - the so called ENERGY PRODUCT : BHmax = Mega Gauss * Oersted (MGsOe or MGO) This regards to the largest possible rectangle area below the Br/Hcb-curve.
For e.g. Neodymium N45 it is 45 MGO.
The values in table (e.g. 43...46) relate to the tolerances in production.
The BH-Diagramm shows how strong an electro magnetic field (H) must be in order de-magnetize a permanent magnet with a field (B).